Charge carrier photogeneration and decay dynamics in the poly(2,7-carbazole) copolymer PCDTBT and in bulk heterojunction composites with PC$_{70}$BM

Minghong Tong, Nelson E. Coates, Daniel Moses,[*] and Alan J. Heeger

Center for Polymers and Organic Solids, University of California, Santa Barbara, California 93106-5090, USA

Serge Beaupré and Mario Leclerc

Departement de Chimie, Université Laval, Quebec City, Quebec, Canada G1K 7P4

Charge carrier photogeneration and decay were studied in poly[N-9″-hepta-decanyl-2,7-carbazole-alt-5,5-(4′,7′-di-2-thienyl-2′,1′,3′-benzothiadiazole)], PCDTBT, and in phase-separated mixtures of PCDTBT with the fullerene derivative [6,6]-phenyl C$_{70}$-butyric acid methyl ester (PC$_{70}$BM). The absorption spectrum of PCDTBT exhibits two distinct absorption bands centered at approximately 400 nm and 600 nm, respectively. In pristine PCDTBT, higher carrier quantum efficiency and lower photoluminescence efficiency are observed following excitation via the higher-energy absorption band. In contrast, in the PCDTBT-fullerene bulk heterojunction material, the carrier generation efficiency is an order of magnitude larger but essentially independent of the excitation wavelength. The photoinduced absorption of PCDTBT:PC$_{70}$BM is interpreted in terms of ultrafast charge transfer, trap filling, and long-lived mobile carriers.

I. INTRODUCTION

Semiconducting polymers continue to be a focus of research because their unique properties offer promise for use in optoelectronics, e.g., in devices such as light-emitting diodes, field-effect transistors, and solar cells.[1–4] The power-conversion efficiency of polymer-based solar cells has steadily increased in recent years, reaching values in excess of 6% using bulk heterojunction (BHJ) films comprised of a semiconducting polymer and [6,6]-Phenyl-C61–butyric acid methyl ester (PCBM) as the charge-separating layer.[5,6] The performance of solar cells made with poly(3-hexylthiophene), P3HT, as the donor polymer is limited by the relatively large band gap of P3HT, (~1.9 eV) which limits the fraction of the solar spectrum that can be harvested ($\lambda \leq 650$ nm). In addition, the relatively small energy difference between the top of the π band (highest occupied molecular orbital, HOMO) of P3HT and the lowest unoccupied molecular orbital of the fullerene acceptor causes the open-circuit voltage to be relatively small, $V_{oc} \approx 0.6$ V.

A new class of semiconducting copolymers has emerged with alternating electron-rich and electron-deficient units in the repeat unit. The synthesis of these novel donor-acceptor structures is motivated by the need to reduce the band gap, and thereby enable better harvesting of solar radiation.[5–12] The molecular structure of poly[N-9″-hepta-decanyl-2,7-carbazole-alt-5,5-(4′,7′-di-2-thienyl-2′,1′,3′-benzothiadiazole)] (PCDTBT) is shown in Fig. 1. In PCDTBT, and more generally in the polycarbazole family,[13] the energy of the HOMO is below that of the HOMO of P3HT. In BHJ mixtures with fullerenes, the deeper HOMO increases the open-circuit voltage and thus increases the power-conversion efficiency of solar cells made with PCDTBT.[5,13,14]

Although the potential utility of these new donor-acceptor (DA) semiconducting copolymers in BHJ solar cells has been demonstrated, relatively little is known about their elec-tronic structure. Specifically, in contrast to the traditional first-generation conjugated polymers,[15] e.g., polyacetylene, polythiophene, and poly(phenylene-vinylene), the PCDTBT absorption spectrum exhibits two distinct absorption bands centered at approximately 400 nm and 600 nm, respectively. The origin of these two absorption bands has not been explored in any detail. The existence of the two strong absorption bands (corresponding to two allowed transitions from the ground state) raises fundamental questions, previously unexplored, regarding the nature of the excited states, relaxation between the excited states, and the ability to photogenerate mobile charge carriers via specific excitation into each of the two excited states.

II. EXPERIMENTAL DETAILS

PCDTBT was synthesized as described in Ref. 13. PCDTBT thin films were spin cast from solution in dichlo-
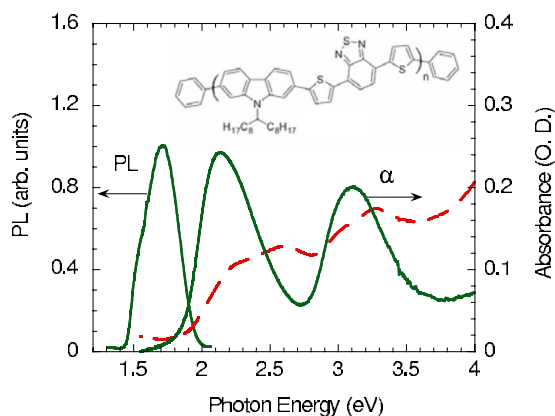

FIG. 1. (Color online) The absorption and photoluminescence spectra of PCDTBT film (solid line) and absorption spectrum of PCDTBT:PC$_{70}$BM bulk heterojunction materials with 1:4 ratio (dashed line). The polymer structure is shown in the inset.

robenzene in a nitrogen glove box with oxygen concentration of 1.5 ppm. The films were cast onto sapphire substrates for the photoinduced absorption (PIA) measurements and onto alumina substrates for steady-state and transient photoconductivity measurements. Film thicknesses were approximately 100 nm, comparable to the absorption depth in the visible spectral region. In order to study the electron transfer and the mobile carrier generation and recombination in the bulk heterojunction system relevant to optimized photovoltaic devices, films were prepared with PCDTBT:PC$_{70}$BM at a ratio of 1:4 (80% PC$_{70}$BM by weight).

The steady-state absorption spectra were measured using a Shimadzu UV-2401 spectrophotometer. The photoluminescence (PL) spectra were obtained using a fluorimeter (Photon Technology International). The transient-absorption (TA) spectra were measured using pulsed laser pump/probe spectroscopy; the Ti:sapphire laser system with a regenerative amplifier provides 100 fs pulses at photon energies of 1.55 eV with 1 mJ per pulse at a repetition rate of 1 kHz. The pump beam was generated using either the second harmonic of the fundamental emission from the Ti:sapphire laser (3.1 eV) or by an Optical Parametric Amplifier (at 2.06 eV). Typical pump intensities ranged from 10–50 μJ/cm^2. The probe beam in the visible and the near-infrared spectral range was obtained from a "white" light continuum, spanning from 1.6 to 2.8 eV, generated by passing a portion of the output from the Ti:sapphire amplifier through a 1-mm-thick sapphire plate. The probe-beam intensity was always less than the pump intensity. The probe pulses were time delayed with respect to the pump pulses using a computerized translation stage capable of time delays up to 1 ns. The beam-spot size on the sample was about 1 mm in diameter for the pump beam and about 0.4 mm diameter for the probe beam. Samples were kept under dynamic vacuum ($<10^{-4}$ mbar) during the PIA and the optoelectronic measurements.

Samples for photoconductivity measurements were configured using the Auston switch geometry, with a 50 μm gap between the 1-mm-wide evaporated aluminum contacts.[16] The Ti:sapphire laser was also used for generating the transient photoconductivity data. For the photoconductivity measurements, the light pulse energy was approximately 10^{-7} J and the beam diameter was about 1 mm. The transient photocurrent was measured using a boxcar system with a sampling head capable of 25 ps temporal resolution. The overall temporal resolution of the transient photoconductivity measurement system was about 100 ps, as indicated by the photocurrent rise time.

Steady-state photoconductivity measurements were carried out using monochromatic light generated from a tungsten lamp source; the incident light beam was mechanically chopped at 170 Hz to enable the use of the standard lock-in amplifier modulation technique. The light was incident normal to the sample surface and had a typical intensity of approximately 100 μW/cm^2. The spectral dependence of the incident beam was determined after each measurement using a calibrated Si photodiode and then used to normalize the PC data.[17]

III. RESULTS AND DISCUSSION

A. Photoconductivity in pristine PCDTBT

For PCDTBT, photoexcitation via each of the two absorption bands is of specific interest. Thus, photoexcitation and recombination of mobile charge carriers were studied as a function of the wavelength of the pump pulse. The photogeneration of mobile carriers was monitored using steady-state photoconductivity action spectra, time-resolved transient photoconductivity as a function of the pump energy, and by measurements of ultrafast time-resolved TA following excitation via the 3.1 eV (400 nm) and the 2.06 eV (600 nm) absorption bands.

Figure 1 shows the steady-state absorption spectrum and the PL spectrum of pristine PCDTBT. The spectrum exhibits two absorption bands with peaks at 2.2 and 3.1 eV. Similar double-peak absorption has been observed in other alternating acceptor-donor copolymers (e.g., the polyfluorene-TBT copolymer[18]). The two absorption peaks were previously attributed to π-π^* transitions with the lower-energy peak associated with intrachain charge transfer.[19]

Note that although the PL spectrum is the same whether the initial absorption is pumped at 3.1 eV or at 2.06 eV, the PL efficiency is slightly higher (by about 10%) when pumped via the lower-energy band (2.06 eV) than via the higher-energy band (3.1 eV). This implies that excitations initially generated from both the 3.1 eV and the 2.06 eV absorption bands decay to form the exciton that subsequently exhibits radiative decay to the ground state by emission at 1.7 eV.

Figure 2(a) shows the steady-state photoconductive internal quantum efficiency (PC-IQE) spectrum exhibited by pristine PCDTBT. Note that there is a significant increase in PC-IQE as the wavelength of the incident radiation moves from the lower-energy band to the higher-energy band.

Figure 2(b) displays the wave forms obtained from the time-resolved photocurrent in pristine PCDTBT after excitation at 3.1 and 2.06 eV. The transient photocurrent was proportional to the light intensity from 0.05 to 2 μJ/pulse. The peak transient photocurrent is approximately a factor of two larger with excitation at 3.1 eV than with excitation at 2.06 eV, a result which is surprising since the mobile carriers would be expected to rapidly relax to the lowest-energy excited state (recall that the PL spectrum is the same whether pumped at 3.1 eV or at 2.06 eV).

The transient and steady-state photoconductivity measurements are fully consistent. The ratio of the time-resolved photocurrents (peak signal from excitation at 3.1 eV divided by that obtained from excitation at 2.06 eV) is close to the corresponding ratio of the steady-state IQE.

Mobile carriers are photogenerated prior to relaxation from the higher-energy band to the lower-energy band and, therefore, prior to the formation of the exciton that yields the PL emission at 1.7 eV. The different efficiencies for mobile carrier generation following excitation at 2.06 and 3.1 eV and the photogeneration of mobile carriers prior to exciton formation imply direct photogeneration of electron-hole pairs (which become polaron pairs after structural relaxation) via π-π^* interband transitions.
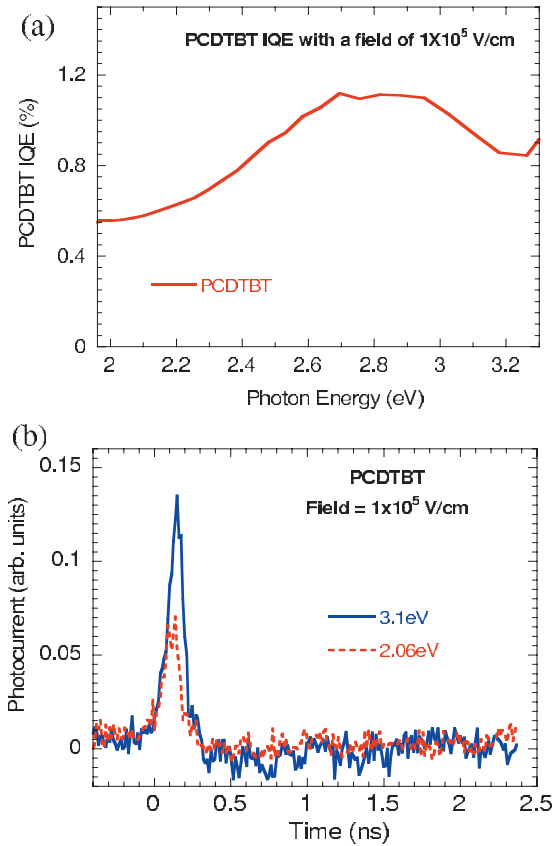
FIG. 2. (Color) (a) Steady-state photoconductivity IQE spectrum of PCDTBT; (b) time-resolved photocurrent in PCDTBT excited at 3.1 and 2.06 eV.

FIG. 3. (Color) (a) Steady-state IQE spectra of PCDTBT:$PC_{70}BM$ (1:4) and (b) time-resolved photocurrent in PCDTBT:$PC_{70}BM$ (1:4) excited at 3.1 and 2.06 eV.

The oscillator strength of the higher-energy absorption band is somewhat smaller than that of the lower-energy absorption band, implying that the transition dipole moment involved in the 2.06 eV transition is somewhat larger. Since the transition dipole moment provides a measure of the redistribution of charge between the ground state and the excited state, one might expect that the larger transition dipole moment associated with excitation at 2.06 eV would lead to a higher yield of mobile photocarriers, in contrast to the experimental observations.

B. Photoconductivity of phase-separated PCDTBT:$PC_{70}BM$ mixtures

The absorption spectrum for the BHJ film (Fig. 1) shows additional absorption from the $PC_{70}BM$ in the 2–3 eV range. For $PC_{70}BM$, the spherical symmetry is broken and the forbidden transitions in the visible part of the spectrum become allowed transitions. The absorption spectrum of PCDTBT:$PC_{70}BM$ films is a superposition of the polymer and the fullerene absorption spectra.

The polymer PL is completely quenched in PCDTBT:$PC_{70}BM$ films. Based on the results of earlier studies of BHJ materials, the PL quenching in the polymer-:fullerene composite results from photoinduced electron transfer from the polymer to the fullerene.[20,21]
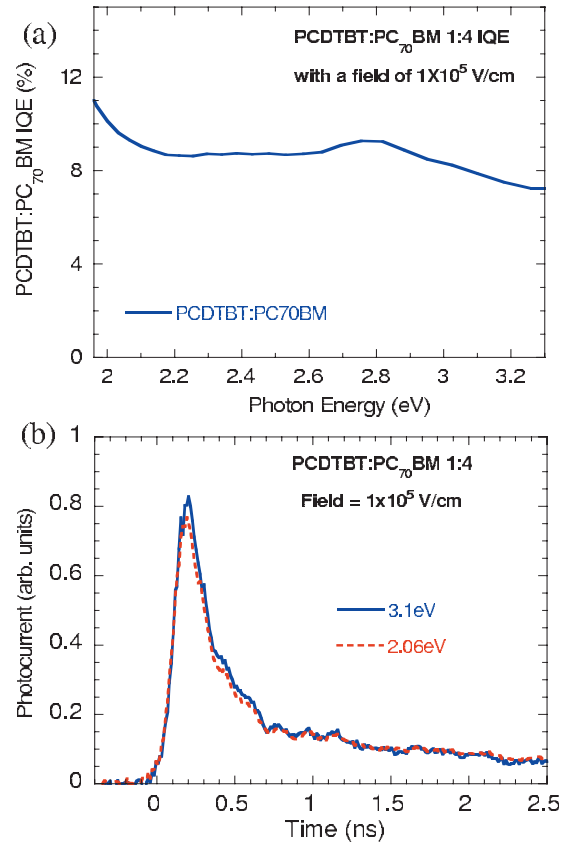
Figure 3(a) shows the steady-state PC-IQE spectrum of the PCDTBT:$PC_{70}BM$ BHJ material with 1:4 weight ratio. The PC-IQE is nearly independent of photon energy. The significant enhancement of the photoconductivity IQE in the composite, by a factor of ~10, compared to that of the pristine polymer is consistent with ultrafast photoinduced charge transfer in the PCDTBT:$PC_{70}BM$.

Figure 3(b) displays the wave forms of the time-resolved photocurrent of the PCDTBT:$PC_{70}BM$ 1:4 material, after excitation at 3.1 and 2.06 eV. The significant difference in peak photocurrent in the pristine material with different excitation energies disappears in the BHJ film, implying that both excited states exhibit ultrafast electron transfer to the $PC_{70}BM$. Because of the photoinduced charge separation, the PCDTBT:$PC_{70}BM$ BHJ composite shows a longer lifetime for photoinduced mobile carriers compared to pristine PCDTBT; a result which is important for efficient photovoltaic-conversion efficiency.

In contrast to the results obtained from pristine PCDTBT, the peak time-resolved photocurrent measured in PCDTBT:$PC_{70}BM$ is nearly independent of excitation wavelength, in agreement with the minimal wavelength dependence of the steady-state PC-IQE of the BHJ material. Although at 2.06 eV, the steady-state photoconductivity is roughly a factor of 16 larger in the polymer:fullerene composite than in the pristine polymer, the peak transient photocurrent is a factor of 11 larger at this wavelength. Similarly,
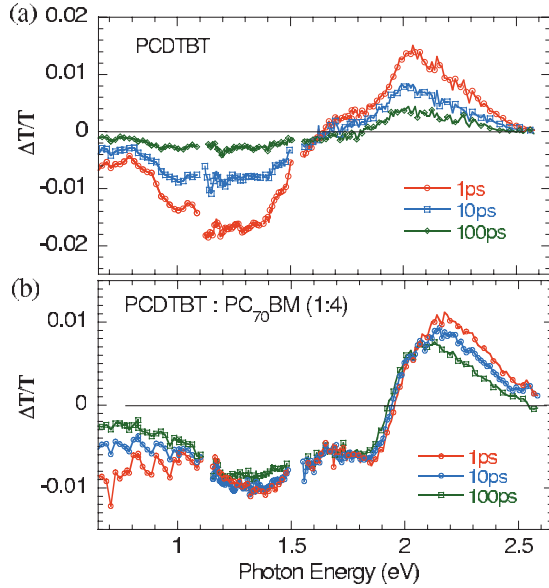
FIG. 4. (Color) (a) Transient-absorption spectra at several delay times excited at 3.1 eV for PCDTBT; (b) PCDTBT:PC$_{70}$BM BHJ film (1:4 ratio).

at 3.1 eV, the steady-state PC-IQE is a factor of nine larger in the composite material whereas in the time-resolved curves, the peak photoconductivity is a factor of six larger in the composite. These differences are explained by noting that the lifetimes of carriers in the polymer:fullerene composite are significantly longer than in the pristine material. The initial decay rate of the transient photoconductivity occurs over a few hundred picoseconds. Considering that in solar cells made with PCDTBT:PC$_{70}$BM, nearly all photogenerated carriers reach the electrodes, the fast initial decay does not result from loss of carriers but rather a decrease in mobility as carriers relax in energy toward the band edges where the states are localized and the mobility is thermally activated.

C. Transient absorption in PCDTBT and PCDTBT:PC$_{70}$BM

Figure 4 shows the TA for pristine PCDTBT and for PCDTBT:PC$_{70}$BM over the spectral range from 0.64 to 2.55 eV measured at three different time delay times following excitation at 3.1 eV. Figure 4(a) shows the spectra for pristine PCDTBT. Three spectral features are evident: (1) a positive signal with maximum at 2.05 eV. (2) A second weaker positive feature near 1.7 eV in the spectral range of the PL. (3) A broad PIA band below about 1.5 eV.

The positive signal with maximum at 2.05 eV results from photobleaching (PB) of the absorption band of the pristine polymer (see Fig. 1). Note that when pumped at 2.1 eV, the PB signal appears at 2.05 eV as well.

The second positive feature near 1.7 eV is coincident in energy with the photoluminescence (see Fig. 1) and decays in less than 100 ps. Therefore, the weak signal near 1.7 eV originates from stimulated emission (SE).

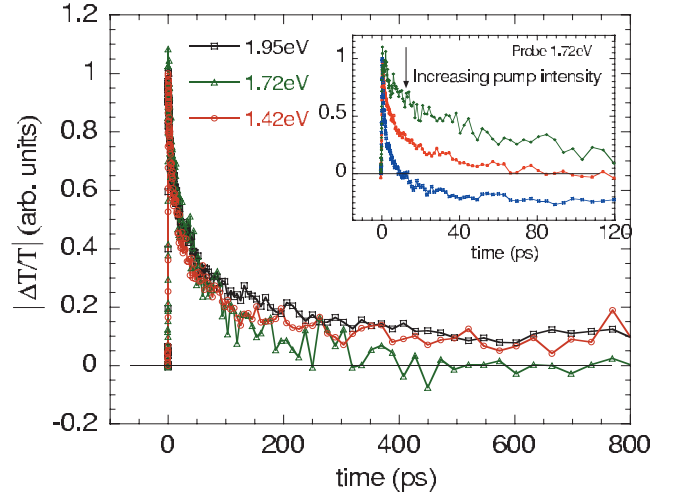The broad photoinduced absorption band below about 1.5 eV is similar to the photoinduced absorption bands com-

FIG. 5. (Color) The transient decay dynamics of PCDTBT at several probe wavelengths for pump wavelength at 610 nm: PB 1.95 eV (square), SE 1.72 eV (triangle), and PA band at 1.42 eV (circle). The inset shows the dynamics of SE band (1.72 eV) at different pump intensities.

monly seen in semiconducting polymers. It is a signature of polaron formation (with associated self-localized states in the energy gap) following photoexcitation.

Figure 5 displays the photoexcitation signal decay in pristine PCDTBT when probed at the three main TA bands (the data are shown in absolute magnitude): 1.95 eV (PB), 1.72 eV (SE), and 1.42 eV (PIA). The TA signal response at 1.95 eV (PB) and 1.42 eV (PIA) exhibit an initial fast decay (~8 ps) followed by a slower component that extends to the nanosecond time regime but the second decay component at 1.72 is relatively short lived and sensitive to the excitation pump intensity. The TA decay rate probed at 1.72 eV at various pump intensities in shown in the inset of Fig. 5; the data indicate that the positive signal (SE) at relatively low intensities decays faster at higher intensities and eventually changes sign to a negative PIA signal.

The TA spectra obtained from PCDTBT:PC$_{70}$BM films with 1:4 weight ratio, presented in Fig. 4(b) are significantly different than the spectrum obtained from the pristine polymer even at delay times as short as 1 ps, consistent with ultrafast photoinduced electron transfer in the BHJ material. Other than the disappearance of the SE band, which is expected since the PL is quenched, we note the following: (1) the TA at 1–1.5 eV has a much longer lifetime, (2) the appearance of a new long-lived TA band centered at 1.8 eV, and (3) the appearance of a new band at 0.7 eV in the BHJ blend, with relatively short lifetime ($\approx$60 ps, see below).

Note that for the polymer:fullerene film with 1:4 component ratio, the amplitude of the new band at 1.8 eV is significantly larger than observed for the 1:1 ratio blend (not shown) at this probe energy.

The longer lifetime of the polaron band (1–1.5 eV) is expected and is consistent with the enhanced photoconductivity in PCDTBT:PC$_{70}$BM. Because of the photoinduced charge separation at the PCDTBT:PC$_{70}$BM interface, recombination of the hole polarons on the PCDTBT is inhibited; hence the longer lifetime.
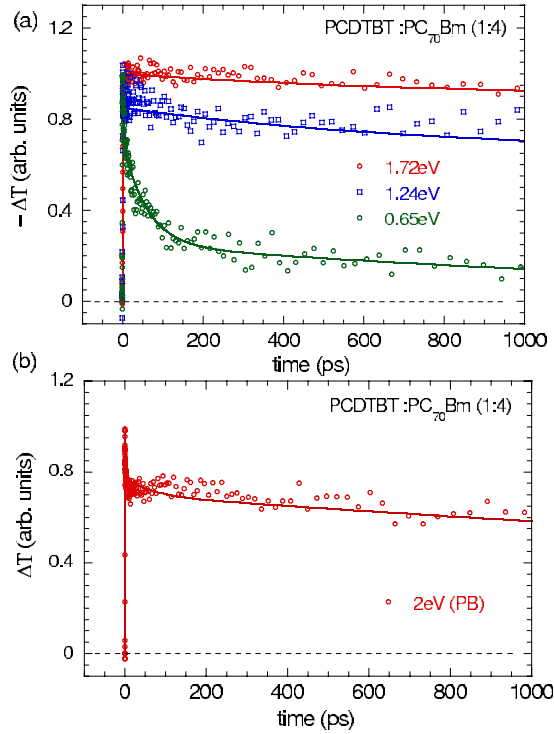
FIG. 6. (Color online) The transient decay dynamics of the PCDTBT:PC$_{70}$BM film at different probe photon energies; the lines are fits to triexponential function, and the obtained lifetimes and weights (given in parenthesis) from the fits for the photoinduced absorption probed at 0.65 eV are: 1.5 ps (30%)+60 ps (45%)+long (25%) and for photoinduced bleaching probed at 2 eV are: 1 ps (22%)+60 ps (8%)+long (70%).

We are not able to unambiguously assign the long-lived band at 1.8 eV in the BHJ blend. It could result from excitation from either the excited state of the PC$_{70}$BM or from the excited state of PCDTBT. Additional PIA measurements on (PC$_{70}$BM)$^-$ and on (PCDTBT)$^+$ using a different donor for the former and a different acceptor for the latter are required to enable a definitive assignment. The fact that the amplitude of this 1.8 eV PIA is larger in the data obtained from the 1:4 composition than from the 1:1 composition suggests, however, that the 1.8 eV PIA arises from the (PC$_{70}$BM)$^-$.

Figure 6(a) shows the TA decay in PCDTBT:PC$_{70}$BM films (1:4) at three-probe wavelengths. The TA signals exhibit significantly longer lifetimes compared to the TA lifetimes obtained from measurements on the pristine film (shown in Fig. 5), consistent with the enhanced photoconductivity in PCDTBT:PC$_{70}$BM.

Note that the new band at 0.7 eV in the BHJ blend appears within 1 ps and that the TA signal at 0.7 eV decays significantly faster than the signal from the higher-energy TA bands. The decay curve can be fit to a sum of three exponentials: 1.5 ps (30% of the initial amplitude), 6 ps (45% of the initial amplitude), and a long tail (>1 ns, 25% of the initial amplitude).

Based on the analysis of Street *et al.*,[22] we assign the 0.7 eV signal to photoinduced absorption from singly occupied interfacial traps. Interfacial traps are expected to become oc-
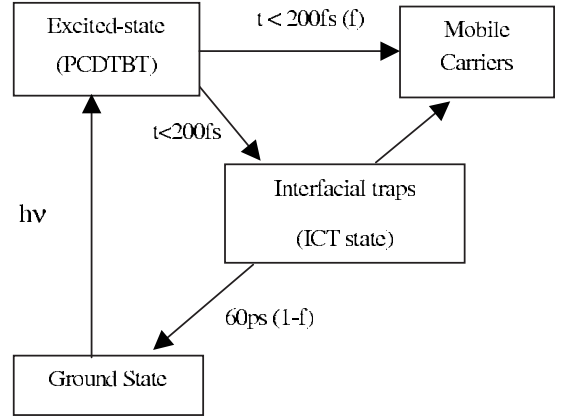

FIG. 7. Schematic of the temporal evolution of the excitations in the PCDTBT:PC$_{70}$BM (1:4) phase-separated BHJ mixtures.

cupied during the initial charge-transfer period, i.e., less than 1 ps. In this model, the fast decay components (1.5 and 60 ps) correspond to relaxation to the ground state following occupation by the second (oppositely charged) carrier. The same 1–1.5 ps decay is observed in the photobleaching signal. The solid line represents the fit by the triexponential function. The long tail indicates that some of the traps remain "active" at long times, perhaps by capturing a long-lived mobile carrier and thereby limiting the lifetime of the mobile holes and electrons in the phase-separated PCDTBT and PC$_{70}$BM, respectively. The identification of the 0.7 eV PIA as resulting from interfacial traps provides a specific interpretation of the "intermediate charge transfer, ICT" state, and the interfacial traps provide a mechanism for interfacial recombination.

Figure 6(b) shows the decay of the photobleaching signal at 2 eV. The solid line in Fig. 6(b) again represents the fit of the triexponential function to the data (see the figure caption for details). The decay of the PB signal measures the recombination decay dynamics of all the photogenerated excitations and therefore enables one to monitor all the recombination losses. The 60 ps component results from carrier recombination via the interfacial traps. This rapidly decaying component has a weight of only 8%, consistent with the high IQE determined from measurements on photovoltaic devices with PCDTBT:PC$_{70}$BM as the charge-separating BHJ layer. The long-lived component of the PB signal arises from the long-lived holes on the PCDTBT, most of which eventually reach the electrode in an illuminated solar cell (long-lived electrons on the PC$_{70}$BM do not contribute to the photobleaching of the PCDTBT absorption).

IV. SUMMARY AND CONCLUSION

In pristine PCDTBT, the carrier photogeneration quantum efficiency is higher and the photoluminescence is lower with photoexcitation via the higher-energy absorption band. The different efficiencies for mobile carrier generation following excitation at 2.06 and 3.1 eV implies direct photogeneration of electron-hole pairs (which become polaron pairs after structural relaxation) prior to the formation of bound exci-

tons. Thus, the data suggest that initial excitations generated via the 2.06 eV π-π^* interband transition in PCDTBT are more spatially confined than excitations generated via the 3.1 eV π-π^* interband transition. These observations indicate the need for comprehensive theoretical studies of the band structure and electronic excitations in DA semiconducting polymers.

The scenario for the time evolution of the excitations in PCDTBT:PC$_{70}$BM, summarized in Fig. 7, is consistent with that proposed in earlier studies of polymer:fullerene BHJ systems;[23–26] the ICT state corresponds to singly occupied interfacial traps. Mobile carriers are generated directly at times less than 150 fs and indirectly (via the interfacial traps) over longer times. The rate of generation of mobile carriers from the interfacial traps is not known.[22] Monomolecular recombination to the ground state (60 ps decay) occurs when a second, oppositely charged carrier is caught in the trap. Over still longer times (beyond the ns regime), mobile carriers can decay by falling into one of the interfacial traps.

The long-time decay reduces the number of carriers on the respective BHJ networks and thereby reduces the power-conversion efficiency of the solar cell. It is important, therefore, to eliminate (or at least minimize) the density of interfacial traps by improved processing during the period over which the spontaneous phase separation occurs.

*Corresponding author; moses@physics.ucsb.edu

[1] S. R. Forrest, Nature (London) **428**, 911 (2004).

[2] G. Malliaras and R. Friend, Phys. Today **58**(5), 53 (2005).

[3] *Handbook of Conducting Polymers*, 3rd ed., edited by T. A. Skotheim and J. R. Reynolds (CRC, Boca Raton, 2007).

[4] G. Dennler, N. S. Sariciftci, and C. J. Brabec, in *Semiconducting Polymers*, edited by G. Hadziioannou and G. G. Malliaras (Wiley, New York, 2007), pp. 455–531.

[5] S. H. Park, A. Roy, S. Beaupre, S. Cho, N. Coates, J. S. Moon, D. Moses, M. Leclerc, K. Lee, and A. Heeger, Nat. Photonics **3**, 297 (2009).

[6] J. Hou, H.-Y. Chen, S. Zhang, R. I. Chen, Y. Yang, Y. Wu, and G. Li, J. Am. Chem. Soc. (to be published).

[7] Y. Liang, D. Feng, Y. Wu, S.-T. Tsai, C. Ray, and L. Yu, J. Am. Chem. Soc. **131**, 7792 (2009).

[8] X. Wang, E. Perzon, F. Oswald, F. Langa, S. Admassie, M. R. Andersson, and O. Inganas, Adv. Funct. Mater. **15**, 1665 (2005).

[9] E. Bundgaard and F. C. Krebs, Sol. Energy Mater. Sol. Cells **91**, 1019 (2007).

[10] D. Mühlbacher, M. Scharber, M. Morana, Z. Zhu, D. Waller, R. Gaudiana, and C. Brabec, Adv. Mater. (Weinheim, Ger.) **18**, 2884 (2006).

[11] J. Peet, J. Y. Kim, N. E. Coates, W. L. Ma, D. Moses, A. J. Heeger, and G. C. Bazan, Nature Mater. **6**, 497 (2007).

[12] Q. Zhou, Q. Hou, L. Zheng, X. Deng, G. Yu, and Y. Cao, Appl. Phys. Lett. **84**, 1653 (2004).

[13] N. Blouin, A. Michaud, D. Gendron, S. Wakim, E. Blair, R. Neagu-Plesu, M. Belletete, G. Durocher, Y. Tao, and M. Leclerc, J. Am. Chem. Soc. **130**, 732 (2008).

[14] N. Blouin, A. Michaud, and M. Leclerc, Adv. Mater. (Weinheim, Ger.) **19**, 2295 (2007).

[15] A. J. Heeger, S. Kivelson, J. R. Schrieffer, and W.-P. Su, Rev. Mod. Phys. **60**, 781 (1988).

[16] D. H. Auston, IEEE J. Quantum Electron. **19**, 639 (1983).

[17] C. Soci, I.-W. Hwang, D. Moses, Z. Zhu, D. Waller, R. Gaudiana, C. J. Brabec, and A. J. Heeger, Adv. Funct. Mater. **17**, 632 (2007).

[18] M. Svensson, F. Zhang, S. C. Veenstra, W. J. H. Verhees, J. C. Hummelen, J. M. Kroon, O. Inganas, and M. R. Andersson, Adv. Mater. (Weinheim, Ger.) **15**, 988 (2003).

[19] K. G. Jespersen, W. Beenken, Y. Zaushitsyn, A. Yartse, M. Anderson, T. Pullerits, and V. Sundstrom, J. Chem. Phys. **121**, 12613 (2004).

[20] N. S. Sariciftci, L. Smilowitz, A. J. Heeger, and F. Wudl, Science **258**, 1474 (1992).

[21] C. H. Lee, G. Yu, D. Moses, K. Pakbaz, C. Zhang, N. S. Sariciftci, A. J. Heeger, and F. Wudl, Phys. Rev. B **48**, 15425 (1993).

[22] R. A. Street, M. Schoendorf, A. Roy, and J. H. Lee (unpublished).

[23] I.-W. Hwang, D. Moses, and A. J. Heeger, J. Phys. Chem. C **112**, 4350 (2008).

[24] I.-W. Hwang, C. Soci, D. Moses, Z. Zhu, D. Waller, R. Gaudiana, C. J. Brabec, and A. J. Heeger, Adv. Mater. (Weinheim, Ger.) **19**, 2307 (2007).

[25] A. Nogueira, I. Montanari, J. Nelson, J. R. Durrant, C. Winder, N. S. Sariciftci, and C. Brabec, J. Phys. Chem. B **107**, 1567 (2003).

[26] H. Ohkita, S. Cook, Y. Astuti, W. Duffy, S. Tierney, W. Zhang, M. Heeney, I. McCulloch, J. Nelson, D. D. C. Bradley, and J. R. Durrant, J. Am. Chem. Soc. **130**, 3030 (2008).